Energy Transfer in the Nanostar: The Role of Coulombic Coupling and Dynamics

Wilfredo Ortiz,[†,‡] Brent P. Krueger,[§] Valeria D. Kleiman,[‡] Jeffrey L. Krause,[†,‡] and Adrian E. Roitberg*[,†,‡]

Quantum Theory Project, University of Florida, P.O. Box 118435, Gainesville, Florida 32611-8435, Department of Chemistry, University of Florida, Gainesville, Florida 32611-7200, and Department of Chemistry, Hope College, Holland, Michigan 49422-9000

Received: February 3, 2005; In Final Form: April 20, 2005

We present a theoretical investigation of energy transfer in the phenylene ethynelene dendrimer known as the nanostar. Data from extensive molecular dynamics simulations are used to model the dynamical effects caused by torsional motion of the phenyl groups. We compare rate constants for energy transfer between the two-ring chromophore and the three-ring chromophore obtained via the Förster model, the ideal dipole approximation (IDA), and the transition density cube (TDC) method, which has as its limit an exact representation of the Coulombic coupling. We find that the rate constants obtained with the TDC are extremely sensitive to the phenyl group rotation, whereas the constants computed with the Förster model and the IDA are not. The implications of these results for the interpretation of recent pump−probe experiments on the nanostar are discussed in detail. Finally, we predict the temperature dependence of the rate constant for energy transfer.

I. Introduction

Dendrimers are synthetic macromolecules that emanate from a central core in a regular, highly branched geometry. They are well-defined structurally and are composed of a core group, followed by successive layers, or generations, of linker-groups, with a branch point at each node. The structure terminates with a variety of possible groups at the periphery. The geometry of dendrimers has been compared to that of a Cayley tree, in the sense that only a single path exists between any two points in the dendrimer, but the number of groups at the periphery increases exponentially as 2^N, where N is the generation.[1,2]

Among their many applications, from catalysis[3−5] to drug-delivery[6] to sensors,[7,8] dendrimers have been proposed as mimics of the light-harvesting system in photosynthesis.[9−17] Their structure is reminiscent of the antenna molecules that are attached to the reaction center. In principle, excitation of any of the terminal units can result in energy transfer to the core, which represents significant signal amplification.

Impressive demonstrations of energy transfer have now been observed in a variety of dendrimeric systems. These include lanthanum[18,19] and porphyrin-cored dendrimers,[20] dye-labeled dendrimers in which the backbone is photochemically inert,[21,22] or has a rigid core,[23,24] and self-assembled structures[25] and films.[26] The research described in this paper is inspired by recent experiments on energy transfer in the phenylene ethynelene dendrimer known as the nanostar (see Figure 1).[27]

In the nanostar, the phenylene ethynelene linker units decrease in size as the generation increases. That is, in generation one the linker is a four-ring system, in generation two a three-ring system, and in generation three a two-ring system. This feature produces an energy gradient in the nanostar, which decreases from the periphery to the core. Energy gradients are present in many biologically active systems, including the elegant light-harvesting antennae of photosynthetic bacteria, as a way of overcoming entropic effects. In the absence of a gradient, energy transfer would occur via a random walk, which would tend to favor transfer to the periphery, rather than to the core.[28] This would increase the probability of energy dissipation to the environment, effectively reducing the transfer yield.

The nanostar is one of the few dendritic structures synthesized with an energy gradient. As a result, this system has has attracted considerable attention. More recently, the Fréchet group prepared a system consisting of a flexible dendrimer scaffold (with aryl ether units) covalently bound to three different dyes.[29] The absorption spectrum of the substituted dendrimer shows the characteristic bands of the individual dyes. Excitation at the high-energy absorption band causes a cascade of energy transfer to a trap. Mullen and co-workers[30,31] synthesized and investigated a rigid polyphenylene scaffold substituted with three different dyes. Again the absorption spectrum of the triad has well separated bands corresponding to the three chromophores and excitation in the high-energy region induces sensitized emission from the trap through a cascade process.

The first experiments on the nanostar showed that excitation of the peripheral groups caused energy transfer to the core with near 100 efficiency.[1,28,32,33] The energy transfer was monitored via the fluorescence from the perylene moiety at the core of the nanostar. Since the fluorescence spectrum of perylene does not overlap with the fluorescence spectrum of the dendrimer, fluorescence acts as a reporter of energy transfer. These experiments demonstrated conclusively that the nanostar acts as a highly efficient, unidirectional energy funnel. The natural question to ask, then, is what is the mechanism of energy transfer.

One clue to the answer of this question comes from the substitution pattern at the branch points of the dendrimer. If the dendrimer were para substituted, conjugated linear molecules would result. The meta substitution in the nanostar allows the dendrimer to reduce steric effects by twisting out of plane. It is also believed to break the conjugation between generations, which localizes the electronic density in subunits.

* To whom correspondence should be addressed.
† Quantum Theory Project, University of Florida.
‡ Department of Chemistry, University of Florida.
§ Hope College.

10.1021/jp050611j CCC: $30.25
Published on Web 05/19/2005

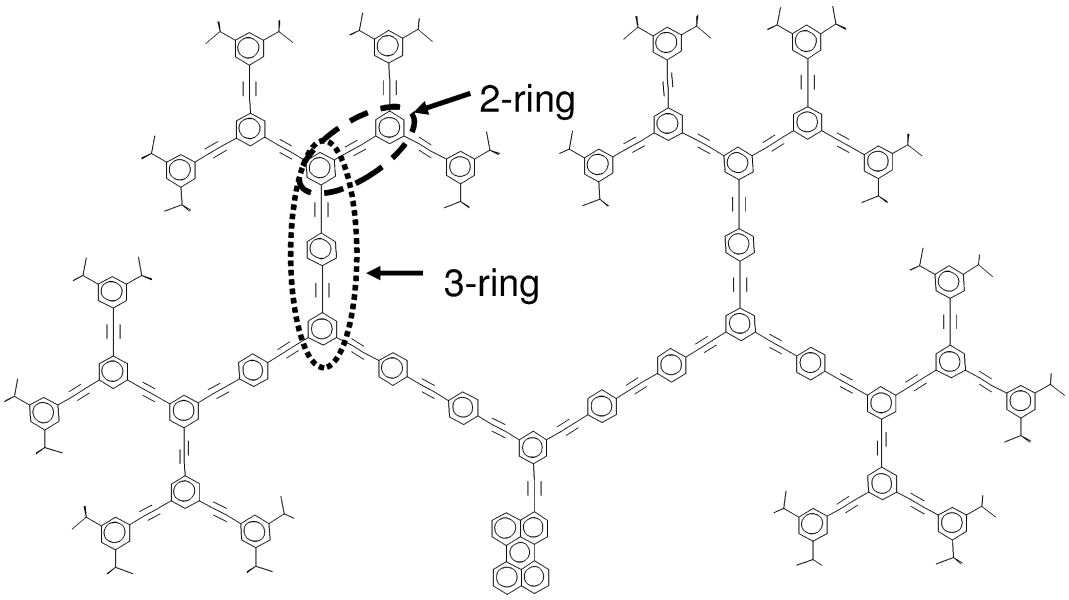

Figure 1. Two-dimensional sketch of the nanostar dendrimer. Examples of the two-ring and three-ring chromophores discussed in the text are noted.

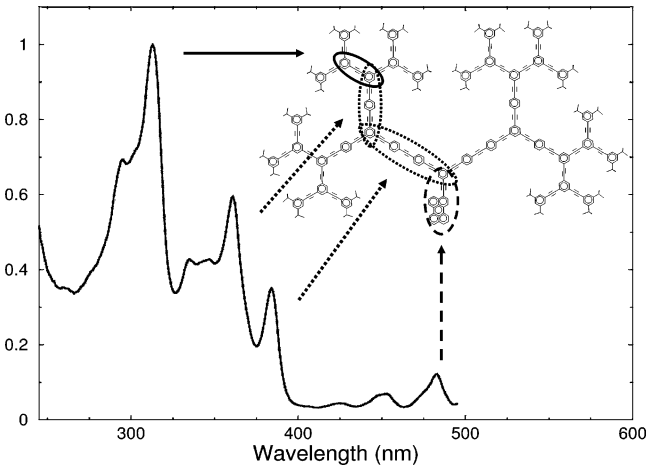

Figure 2. Absorption spectra of the nanostar at 77 K. Unpublished data courtesy of Joseph S. Melinger (NRL).

Evidence that conjugation does not delocalize the electronic density over the entire backbone can be seen in the low-temperature absorption spectrum of the nanostar (see Figure 2). Peaks in the spectrum can be identified clearly with the one-, two-, three-, and four-ring systems. The intensity of the absorption spectrum has been shown to scale linearly with the number of conjugated units, which is consistent with the model of localized excitations,[1,17] Additional evidence comes from both experimental and theoretical investigations.[33−36]

Using a time-correlated single photon counting technique to measure excited-state fluorescence lifetimes, Swallen et al.[28] determined an upper limit to the ensemble-averaged trapping time from the lowest (4-ring) state to the core of about 10 ps. For excitation from the periphery, they estimated an upper limit to the trapping time of 270 ps. Further experiments by Kleiman et al.[35] using degenerate pump−probe spectroscopy to measure the relaxation time between the 2-ring and 3-ring intermediates found a biexponential decay with two components, 3.0 ± 0.5 and 14 ± 2.5 ps, and subpicosecond decays for the 3- and 4-ring systems. Modeling the results with Förster theory, (described in detail below) by Kleiman et al.[35] and Devadoss et al.,[32] produced at best qualitative agreement with experiment.

Theoretically, Tada et al.[37] performed extensive molecular orbital calculations that showed strong localization of the orbital density in the chromophores. Mukamel and co-workers used a collective electronic oscillator approach to calculate the absorption spectrum of the nanostar.[2] Implicit in this approach is the division of the optical excitation into weakly interacting chromophores separated by the meta branch points. Spectra calculated with this technique are consistent with the experimental spectra. Mukamel and co-workers used the same method to calculate frequency-gated fluorescence spectra.[38] The time-dependent doorway wave packets are again consistent (after an initial short-lived coherence) with a picture in which the energy transfers via population migration down the energy funnel. Mukamel and co-workers also developed a Frenkel exciton Hamiltonian to describe the optical and transport properties of the nanostar.[34] Their calculated absorption spectra are in excellent agreement with experiment.

The assumption that energy transfer occurs via excitations localized on chromophores separated by meta substitution was disputed by Martínez and co-workers.[39,40] They point out that, although meta substitution blocks conjugation in the ground state, this is not necessarily the case in the excited state. Using high-level quantum chemistry calculations of highly symmetric model compounds related to the nanostar, they find strong variability of the electronic coupling with molecular geometry. In particular, they demonstrate that the coupling changes dramatically from the absorbing geometry (in which the coupling is small) to the emitting geometry (in which the coupling is large). To describe the relaxation-induced coupling, they extend a model due to Harcourt in which the through-bond and through-space contributions are augmented with "ionic", or charge-transfer contributions.[41]

In the nanostar, there is also a distinct possibility of direct energy transfer from the periphery to the core. This is unlikely because of the large distances involved, and the small electronic overlap between the peripheral units and the core. To investigate this possibility, experiments are underway in the Kleiman group to determine the contributions of sequential versus direct energy transfer.

In this work, we perform molecular dynamics simulations on the nanostar to elucidate the role of structural changes on

the dynamics at finite temperature. We model the Coulombic contribution to the energy transfer between the 2-ring and 3-ring chromophores using the ab initio transition density cube (TDC)[42] method to calculate the electronic couplings and energy transfer rates beyond the dipole approximation. Finally, we estimate the effect of temperature on the energy transfer rates.

II. Method

Modeling of dendrimers is challenging because they are large fluxional molecules. Changes in the geometry of the molecule can cause large variations in transport properties.[32,43] To obtain structural information about the nanostar, we performed large-scale molecular dynamics simulations. The results of these simulations are used as input for energy transfer calculations, as described below.

The molecular dynamics simulations were performed using TINKER (version 3.9).[44] For the minimization and subsequent dynamics simulation, the interparticle interactions were modeled with the MM3 force field, which has been parametrized to treat organic systems.[45−47] In the nanostar (see Figure 1), one important feature is the presence of phenyl groups connected to ethynelene units. The experimental value for the rotational barrier in diphenylethynelene is 0.6 kcal/mol.[48−50] The original MM3 rotational barrier is 0.001 kcal/mol. To correct this deficiency, the TINKER force field was modified to better reflect the experimental value. Specifically, the force constant for the torsion angle between atom type 50−50−4−4 and 50−4−4−50 was changed from 0.001 to 0.65 kcal/mol, where atom type 50 represents a carbon atom in a phenyl ring, and atom type 4 represents a carbon atom in an alkyne.

The initial structure of the nanostar was constructed as a fully extended molecule and then minimized until the root-mean-square gradient of the energy converged to less than 0.01 kcal/mol/Å. Following the structure minimization, molecular dynamics simulations were performed at 300 K for 20 ns. Snapshots of the molecular geometry were saved every 10 ps. The time step in the dynamics was 1 fs. The propagation was performed with the velocity Verlet-based stochastic method, and the thermostat algorithm was the Berendsen bath coupling method. The simulations assumed a constant dielectric continuum of 1.5, which, in the Allinger MM3 force field, corresponds to the vacuum. The solvents used in the experiments are typically dichloroethane or *n*-hexane, both of which have relatively low dielectric constants. The use of a constant dielectric in the simulations, while somewhat crude, should not alter the qualitative trends reported in this work.

A. Energy Transfer. Traditionally, energy transfer between chromophores is interpreted using models proposed by Dexter and Förster. In the Dexter, or through-bond, model, energy transfer results from a simultaneous exchange of electrons from the excited state of the donor to the excited state of the acceptor, and the exchange of an electron from the ground state of the acceptor to the ground state of the donor. The Dexter model requires strong donor−acceptor orbital overlap and is short range, with an exponential dependence on the interchromophore distance.[41,51,52]

In the Förster, or through-space model, energy transfer occurs via a Coulombic dipole−dipole interaction. The rate constant in the Förster model is given by[53]

$$k_{ET}^{F} = \frac{9000 \ln(10)\, \kappa^2 \phi_D J}{128 \pi^5 n^4 N_A \tau_D R^6} \tag{1}$$

where κ^2 is the orientation factor of the dipole moments, ϕ_D is the donor quantum yield, J is the overlap integral between the donor emission spectrum and the acceptor absorption spectrum, n is the index of refraction of the solvent, N_A is Avogadro's number, τ_D is the donor lifetime in the absence of the acceptor, and R is the distance between the centers of donor and acceptor transition dipoles.

Förster theory has been used with great success in a wide variety of systems. However, its application in dendrimers is problematic for several reasons. For one, dendrimers have many donors that can transfer energy to a common acceptor. Each of these donors may have vastly different chemical environments and relative geometries. Depending on the structure of the dendrimer, terminal units in the same generation may have a broad distribution of distances from the core. Due to the R^{-6} distance dependence, the implications of this distribution can be large, as we showed recently in the poly(benzylphenyl ether) (PBPE) dendrimer.[43] In the PBPE system, the comparatively rare event of peripheral units backfolding to the core dominates the dynamics of energy transfer. Some of these difficulties can be overcome by performing experiments at the single-molecule level, as has been demonstrate recently.[54−56]

Compared to PBPE, the nanostar is fairly rigid, so backfolding is not an important issue. However, the chromophores in the nanostar are adjacent, which brings the validity of the Förster formula (and its underlying ideal point dipole approximation, IDA) into question. Another potential deficiency in the Förster method is in the treatment of dynamical variations of the dipole orientations at nonzero temperature. Although several parameters of the model, κ^2, J, τ, and ϕ_D depend on the donor or acceptor electronic structure, most applications of the model treat κ^2 as the only variable. With just a single variable, the Förster formula cannot be expected to capture the effects of dynamics adequately.

To investigate the role and magnitude of these potential deficiencies, we consider energy transfer between 1,2-diphenylethyne (or diphenylacetylene) and 1,4-bis(phenylethynyl) benzene, as models of the two-ring and three-ring chromophores, respectively. We compare the energy transfer rates as a function of the distance between the chromophores obtained via the Förster method, the ideal dipole approximation, and an approximation to the full Coulombic interaction.

The rate of energy transfer between two chromophores, in the weak coupling limit, is defined as

$$k_{ET} = \frac{4\pi^2 J}{h^2 c} |V^{Coul}|^2 \tag{2}$$

where h is Planck's constant, c is the speed of light in a vacuum, J is the spectral overlap between the absorption spectrum of the acceptor and the fluorescence spectrum of the donor, and V^{Coul} is the Coulombic coupling between the two chromophores. Note that J in this formula is defined differently than J in eq 1. In eq 1 J is in units of cm^6/mol, whereas in eq 2, J has units of cm. The complete representation of the Coulombic coupling is

$$V^{Coul} = 2 \int \psi_D^* \psi_A \frac{1}{r_{12}} \psi_D \psi_A^* \, d\tau \tag{3}$$

where ψ_D^* and ψ_D are the excited and ground-state wave functions of the donor chromophore, ψ_A^* and ψ_A are the excited and ground-state wave functions of the acceptor chromophore, and the integration is over all space. The full Coulomb interaction can be approximated as the sum of all the multipole interactions

$$V^{\mathrm{Coul}} = V^{\mathrm{mult}} = V^{\mathrm{d-d}} + V^{\mathrm{d-q}} + V^{\mathrm{q-d}} + \cdots \quad (4)$$

between the transition densities of the two chromophores involved in the energy transfer process.

To calculate V^{Coul}, we use a method developed previously called the transition density cube method (TDC).[42] We should note that an alternative method for calculating V^{Coul} has been presented recently.[57] Note, too, that the Förster formula can be represented as the dipole−dipole term, $V^{\mathrm{d-d}}$, the first term in the multipole expansion.

In the TDC method,[42] the transition density of a molecule is given by

$$M_N^{\mathrm{eq}}(\mathbf{r}) = \psi_N \psi_N^* \quad (5)$$

where N is either D, for the donor, or A, for the acceptor. The excited-state wave functions of the donor (2-ring chromophore) and acceptor (3-ring chromophore) are calculated using Q-Chem (version 2.0) at the configuration interaction level with single excitations from a spin-restricted Hartree−Fock reference determinant. We use a 3-21G* basis and tested for convergence with a larger basis (6-31G*).

In the TDC method, the transition density is discretized onto cubes defined by integrating the product of the ground and excited-state wave functions on a three-dimensional grid

$$M_N^{\mathrm{eq}}(x, y, z) = V_\delta \int_z^{z+\delta_z} \int_y^{y+\delta_y} \int_x^{x+\delta_x} \psi_{N\mathrm{g}} \psi_{N\mathrm{e}}^* \, \mathrm{d}x \, \mathrm{d}y \, \mathrm{d}z \quad (6)$$

where δ_α defines the grid size of the density cube and $V_\delta = \delta_x \delta_y \delta_z$ is the volume element. In this work, each TDC requires 125 000 elements to converge the results to ±1%, giving a volume of ~0.3 Bohr^3 for each element.

The electronic coupling between the donor and acceptor is computed as

$$V^{\mathrm{Coul}} \cong \sum_{i,j} \frac{M_{\mathrm{D}}^{\mathrm{eg}}(i)\, M_{\mathrm{A}}^{\mathrm{eg}}(j)}{4\pi\epsilon_0 r_{ij}} \quad (7)$$

where $M_{\mathrm{D}}^{\mathrm{eg}}(i)$ and $M_{\mathrm{A}}^{\mathrm{eq}}(j)$ are the transition densities for the donor (D) and acceptor (A). The result of computing V^{Coul} with eq 7 is a representation of the exact Coulombic interaction (for a given estimate of ψ and ψ^*) in the limit that the number of cubes goes to infinity. Note that this equation is simply a discretized version of eq 3.

III. Results and Discussion

The basic assumption of the Förster model is the ideal dipole approximation (IDA), which should fail at short interchromophore distances, R. To assess the magnitude and range of validity of the model, we computed the Coulombic coupling between the two-ring and three-ring chromophores with the IDA and the TDC methods. In these calculations, the distance between the chromophores was varied, maintaining the transition moments parallel to each other. Figure 3 shows the results as a function of R. At 10 Å, the difference between the IDA and the TDC method is large, whereas as the separation between the chromophores increases, the difference decreases. As expected, at large distances, the dipoles approach point dipoles, and the agreement between IDA and the TDC is perfect.

In the nanostar, the separation between the two-ring and three-ring chromophores ranges from 9.1 to 15.1 Å, which, as seen in Figure 3, is exactly the range in which the Förster model becomes questionable.

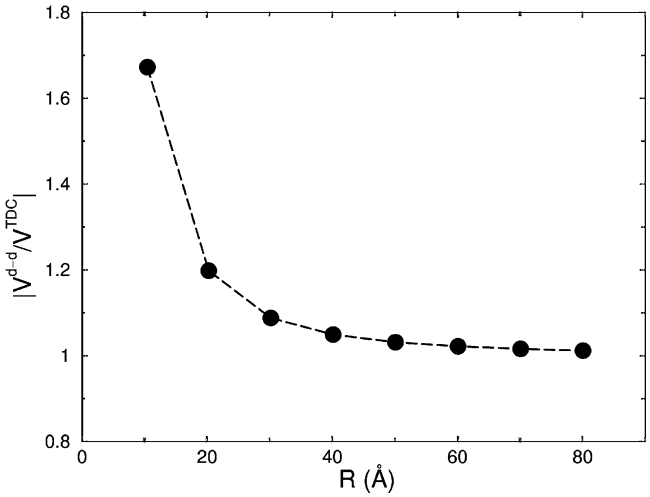

Figure 3. Ratio of the Coulombic coupling between the two-ring and three-ring chromophores, as calculated with the IDA method ($V^{\mathrm{d-d}}$) and the transition density cube method (V^{TDC}).

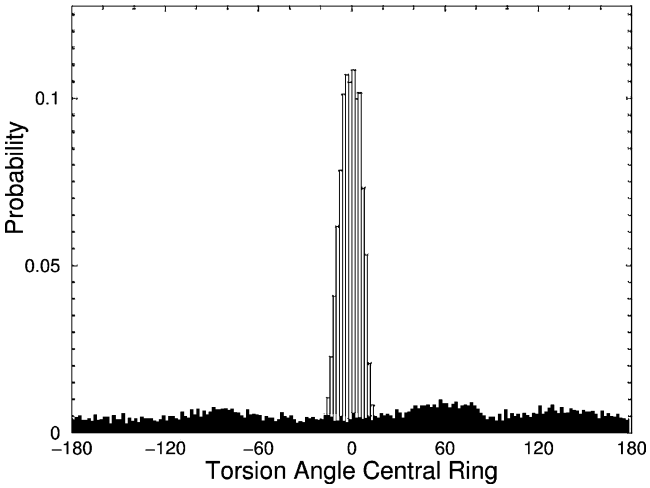

Figure 4. Distribution of the torsion angle of the middle phenyl group in the three-ring chromophore. The filled bars correspond to dynamics at 300 K and open bars correspond to dynamics at 10 K.

A further reason to mistrust simple applications of the Förster model is due to the possible effects of changes in the geometry of the nanostar. At least two types of geometry changes are relevant for the efficiency of energy transfer. One involves dynamical changes in the relative orientations of the donor and the acceptor, which would affect the parameters R and κ^2. A second involves dynamics within the donor and acceptor themselves. As observed in the molecular dynamics simulations, the nanostar is rather rigid, so the effects of large-scale geometry changes (at least between the two-ring and three-ring chromophores) are small.

Although the overall structure of the nanostar is rigid, the phenyl rings are free to rotate around the ethynelene bonds. Figure 4 shows the distribution of torsion angles for the center ring of the three-ring chromophores at two different temperatures, 10 and 300 K. At low temperature, the rings lie essentially in the same plane. At room temperature, the torsional barrier is of the same order as kT, and the rings rotate freely. As might be expected, this change in geometry has a significant effect on the transition density.

Figure 5 shows the transition densities (as isodensities at levels of ±0.01 e, where e is the charge on an electron) for the

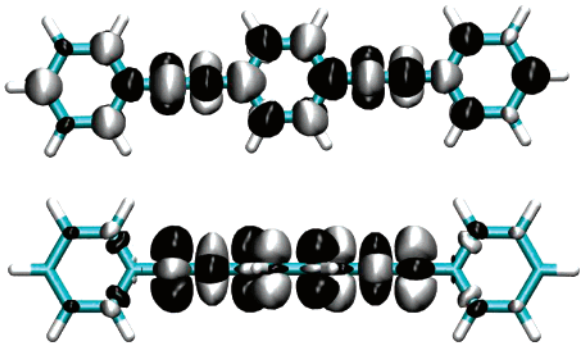

Figure 5. Transition density of the 3-ring chromophores in two different conformations, planar (top) and with the center phenyl ring twisted 90° out of the plane (bottom). The calculated dipole moments are 11.8 D for the planar configuration and 6.5 D for the twisted configuration.

planar structure and the structure in which the center ring is rotated by 90° out of the plane. The planar geometry has a transition density distributed over the entire chromophore, whereas the off-planar geometry shows a transition density concentrated mostly on the central region involving the phenyl ring and two ethynelene groups. This difference between the transition densities translates directly into marked changes in the Coulombic coupling. The rotation around the central angle also has a substantial effect on the magnitude of the electronic transition dipole moment for the 3-ring chromophore.

Note that rotation of the outer ring in the 2-ring chromophore is also possible. However, rotation of this ring is hindered by bulky groups at the periphery of the dendrimer. As a result, the outer ring does not rotate freely at room temperature, and the effects of this rotation were not considered here.

Figure 6 shows energy transfer rates between the 2-ring and 3-ring chromophores as a function of the torsion angle of the central ring in the 3-ring chromophore. The rates are computed in three different ways. One uses the Förster method (eq 1), with J fixed, and the values of κ^2 and R fixed at 2.7 and 9 Å, respectively, which is one of the set of values assumed previously for the nanostar.[35] A second method uses the IDA, which is the first term in the multipole expansion in eq 4, computed as

$$|V_{\mathrm{IDA}}|^2 = \left(\frac{\kappa}{4\pi\epsilon_0 R^3}\right)^2 \langle\psi_{\mathrm{D}}^*|\mu_{\mathrm{D}}|\psi_{\mathrm{D}}\rangle^2 \langle\psi_{\mathrm{A}}^*|\mu_{\mathrm{A}}|\psi_{\mathrm{A}}\rangle^2 \qquad (8)$$

The final method uses the TDC. Note that there is no inherent reason in the Förster method to use fixed values of the parameters. Fixing κ^2 is, however, a common practice in the interpretation of experimental data.

As can be seen in the figure, the Förster values and the IDA are in rather good agreement. Although there is no explicit dependence on the torsion angle in the Förster formula (though an implicit dependence exists through the parameter J), the IDA does contain an explicit dependence on the angle in the factor $\langle\psi_{\mathrm{A}}^*|\mu_{\mathrm{A}}|\psi_{\mathrm{A}}\rangle$. These results are a warning that dynamical effects must be considered even in simplified applications of Förster theory.

In contrast to the Förster and IDA results, the TDC shows a strong dependence on the torsion angle. In fact the rate constant at 90° is nearly a thousand times smaller than that at 0°. Since, as seen in Figure 4, the distribution of angles at room temperature is nearly flat, the ring rotation is a factor that must be included when modeling energy transfer in the nanostar. Correcting the Förster formula by using κ^2 as a fitting parameter

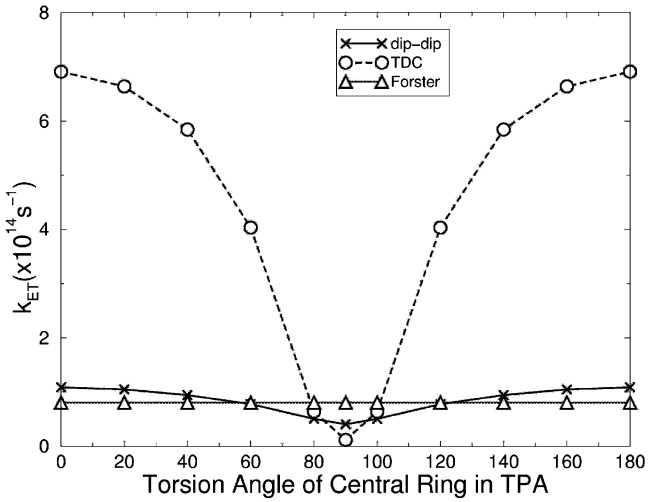

Figure 6. Rate constant for energy transfer as a function of the rotation of the middle phenyl group in the three-ring chromophore, as calculated with the Förster method (triangles), the IDA (crosses), and the transition density cube method (circles).

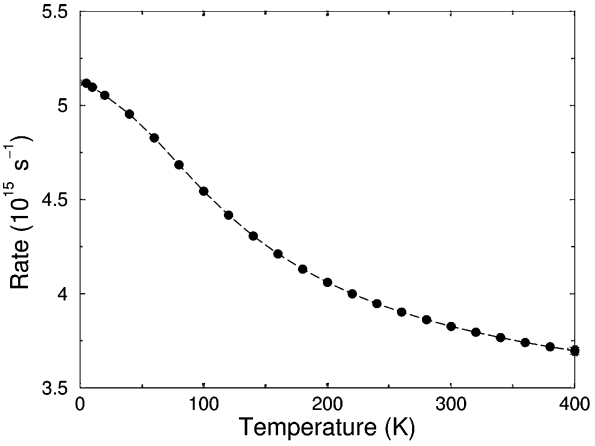

Figure 7. Rate constant for energy transfer between the 2-ring and 3-ring chromophores as a function of temperature with fixed J. The temperature dependence is due only to the rotation of the middle phenyl ring of the three-ring chromophore.

might bring the Förster results into better agreement with the IDA, but would not be sufficient to match the more accurate coupling reflected in the TDC results. However, as seen in Figure 5, the dominant effect of the torsional motion is variation in the transition densities, so the overlap integral J would likely be a sensitive parameter.

Finally, we can use the dependence of the rate constant on the torsion angle to predict the dependence of the rate constant on temperature. For the transition between the two-ring and three-ring chromophores, the dependence can be written (see the Appendix for details of the derivation)

$$\langle k_{\mathrm{ET}}\rangle_{\mathrm{T}} = \frac{A\,B}{\int \exp(-\beta U(\phi))\,\mathrm{d}\phi}\left[\frac{\mathrm{erf}(\sqrt{C})\sqrt{\pi}}{\sqrt{C}}\right] \qquad (9)$$

where A is proportional to the overlap integral (J), B is a fitting parameter, C is a constant inversely proportional to the temperature, $\beta = 1/kT$, and $U(\phi)$ is the torsional function from the modified MM3 force field. Equation 9 shows that at fixed J the rate of energy transfer between the 2-ring and 3-ring chromophores should decrease with increasing temperature (see Figure 7). The reason for this dependence is that at low temperatures the torsion angle between the phenyl rings in the

3-ring system is peaked near zero, where the transition dipole is maximum.

However, the overlap integral, *J*, also depends (in a nontrivial way) on the temperature, which leads to a competition between geometric factors and overlap effects. To estimate the magnitude of this effect, we calculated the overlap integral, *J*, at two different temperatures, 77 and 300 K. For the 300 K values, we used experimental data for the excitation (absorption) spectrum of the 3-ring chromophore[58] and the fluorescence spectrum of the 2-ring chromophore.[59] For the 77 K values, we used experimental data for the excitation spectrum,[60] and assumed that the fluorescence spectrum is independent of temperature.[61] At 300 K, we find that the value of *J* is twice that at 77 K, which implies that the rate constant for energy transfer should be twice as fast at high temperature than at low temperature. On the basis of the combination of results for torsion and *J*, we predict a small increase in the rate constant with temperature. Further modeling of the temperature effect is required to determine which of these competing trends dominate. Experimental determination of the dependence of the rate on temperature is in progress.

IV. Conclusions

As has been stated previously, attempts to apply Förster theory to the nanostar are "fraught with difficulty".[32] In this work, we analyze the causes and effects of some of these difficulties. First, using an isolated two-ring chromophore and three-ring chromophore as models of the donor and acceptor studied in the work of Kleiman et al.,[35] we showed that the Förster model underestimates the rate of energy transfer by about a factor of 7. This is a result of the inadequacy of the Förster method at short interchromophore distances. For such distances, a treatment of the exact Coulombic interaction, such as that provided by the transition density cube method, is crucial.

A second difficulty with the traditional Förster model is that it neglects dynamical effects. In the nanostar, the rapid flipping of the phenyl groups at room temperature causes large changes in the transition densities and hence the rates. Again, a full treatment of the Coulombic interaction is necessary to correct this difficulty. Data from the molecular dynamics about the distribution of the torsion angles allowed us to make a prediction of the effect of temperature on energy transfer.

Finally, we must also state that rates calculated with the TDC are correct only if the energy transfer mechanism involves purely through-space Coulombic interaction of isolated chromophores. If through-bond or other mechanisms are operative, the TDC will fail to capture the relevant physics.[39−41] The TDC method will also fail if the energy transfer occurs from many strongly coupled donors to a single acceptor.[62] The best way to prove the assertions made in this paper is via comparison to experimental data. Such comparisons are underway.

The extant experimental data for energy transfer between the two-ring and three-ring chromophores show two transients, one fast (3.0 ps) and one slow (14 ps). The slow component is consistent with the predictions of Förster theory. The qualitative agreement with experiment could perhaps be improved by the use of the TDC and data from molecular dynamics. The faster signal may be consistent with through-space Coulombic coupling, but may also be an indication of the presence of additional mechanisms. Further investigations of this issue are underway. Also underway are experiments using multiccolor pump−probe spectroscopy to create a complete map of the energy pathways in the nanostar.

Acknowledgment. We thank Dr. C.-P. Hsu for useful discussions and comments. This work was partially supported by the Department of Energy through grant DE-FG02-02ER45995 (J.L.K. and A.E.R.), Research Corporation, through Cottrell College Science Award CC5479 (B.P.K.), and the Towsley Foundation (B.P.K.).

V. Appendix A

As discussed in the text (see eq 8), the observed dependence of the rate constant for energy transfer on the rotation of the middle ring of the three-ring chromophore can be used to estimate a temperature dependence of the rate constant. At a given temperature, the average rate constant can be written

$$\langle k_{ET}\rangle_T = \int_0^{\pi} k_{ET}(\phi)\, P(\phi)\, d\phi \tag{10}$$

where $k_{ET}(\phi)$ is defined as

$$k_{ET}(\phi) = \frac{4\pi^2 J}{h^2 c}|V^{Coul}(\phi)|^2 \tag{11}$$

In general, the probability to observe a certain angle, ϕ, is

$$P(\phi) = \exp(-\beta U_{Tors}(\phi))/\int_0^{\pi} \exp(-\beta U_{Tors}(\phi))\, d\phi \tag{12}$$

where $\beta = 1/kT$. The functional form of U_{Tors} used in the molecular dynamics force field is

$$U_{Tors}(\phi) = \frac{V_2}{2}(1 - \cos 2\phi) \tag{13}$$

where V_2 is a constant. The integral in the denominator of eq 12 can be written in the form

$$\int_0^{\pi} \exp(-z(1 - \cos 2\phi))\, d\phi \tag{14}$$

where z is defined as

$$z = \frac{\beta V_2}{2} \tag{15}$$

After a change of variable ($x = 2\phi$) the resulting integral can be solved as

$$\frac{1}{2}\int_0^{2\pi} \exp(-z)\exp(z\cos x)\, dx = \pi I_0(z)\exp(-z) \tag{16}$$

where I_0 is a modified Bessel function.

Given values of β and V_2, the above equation can be used directly to calculate $P(\phi)$. To determine $\langle k_{ET}\rangle_T$ in eq 10 we require a model for $k_{ET}(\phi)$. This can be determined from the dependence of the rate on the angle as computed with the TDC. To do this, eq 10 can be recast as

$$k_{ET}(\phi) = A|V_{TDC}^{Coul}(\phi)|^2 \tag{17}$$

where

$$A = \frac{4\pi^2 J}{h^2 c} \tag{18}$$

The dependence on the angle can be fit with an analytical function of ϕ. One that works well (see Figure 8) for this case is

$$|V_{TDC}^{Coul}(\phi)|^2 \approx B|\cos\phi| \tag{19}$$

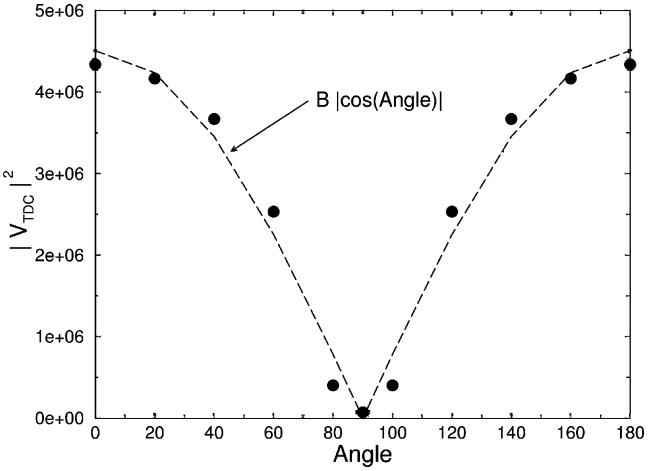

Figure 8. Coulombic coupling squared between the three-ring and two-ring chromophores, as calculated with the transition density cube method (circles). The angle is the torsion angle of the middle benzene ring in the three-ring chromophore. An angle of 0° or 180° corresponds to a configuration in which all three rings are planar, whereas an angle of 90° corresponds to a configuration in which the middle ring is perpendicular to the plane containing the remaining rings. The dashed curve is the fit to the calculated data points as described in the text.

Then

$$k_{ET}(\phi) = AB\,|\cos\phi| \tag{20}$$

With this approximation, eq 9 can be written as

$$\langle k_{ET}\rangle_T = \frac{AB}{\int \exp(-\beta U(\phi))\,d\phi}\int_0^{\pi} |\cos\phi|\,\exp(-C\sin^2\phi)\,d\phi \tag{21}$$

which can be evaluated as

$$\langle k_{ET}\rangle_T = \frac{AB}{\int \exp(-\beta U(\phi))\,d\phi}\left[\frac{\mathrm{erf}(\sqrt{C})\sqrt{\pi}}{\sqrt{C}}\right] \tag{22}$$

where

$$C = \frac{V_2}{k_B T} \tag{23}$$

and the constant B is varied to best fit the calculated TDC points.

References and Notes

(1) Kopelman, R.; Shortreed, M.; Shi, Z.-Y.; Tan, W.; Xu, Z.; Moore, J. S.; Bar-Haim, A.; Klafter, J. *Phys. Rev. Lett.* **1997**, *78*, 1239−1242.
(2) Tretiak, S.; Chernyak, V.; Mukamel, S. *J. Chem. Phys. B* **1998**, *102*, 3310−3315.
(3) Bosman, A. W.; Janssen, H. M.; Meijer, E. *Chem. Rev.* **1999**, *99*, 1665−1688.
(4) Hecht, S.; Fréchet, J. M. J. *Angew. Chem., Int. Ed.* **2001**, *40*, 74−91.
(5) Twyman, L. J.; King, A. S. H.; Martin, I. K. *Chem. Soc. Rev.* **2002**, *31*, 69−82.
(6) Boas, U.; Heegaard, P. M. H. *Chem. Soc. Rev.* **2004**, *33*, 43−63.
(7) Crooks, R. M.; Ricco, A. J. *Acc. Chem. Res.* **1998**, *31*, 219−227.
(8) Miller, L. L.; Kunugi, Y.; Canavesi, A.; Rigaut, S.; Moorefield, C. N.; Newkome, G. R. *Chem. Mater.* **1998**, *10*, 1751−1754.
(9) Adronov, A.; Fréchet, J. M. J. *Chem. Commun.* **2000**, *18*, 1701−1710.
(10) Balzani, V.; Ceroni, P.; Maestri, M.; Saudan, C.; Vicinelli, V. *Top. Curr. Chem.* **2003**, *228*, 159−191.
(11) Aida, T.; Jiang, D.-L.; Yashima, E.; Okamoto, Y. *Thin Solid Films* **1998**, *331*, 254−258.
(12) Hahn, U.; Gorka, M.; Vögtle, F.; Vicinelli, V.; Ceroni, P.; Maestri, M.; Balzani, V. *Angew. Chem., Int. Ed.* **2002**, *41*, 3595−3598.
(13) Precup-Blaga, F. S.; Garcia-Martinez, J. C.; Schenning, A. P. H. J.; Meijer, E. W. *J. Am. Chem. Soc.* **2003**, *125*, 12953−12960.
(14) Bar-Haim, A.; Klafter, J. *J. Lumin.* **1998**, *76*−*77*, 197−200.
(15) Momotake, A.; Arai, T. *Polymer* **2004**, *45*, 5369−5390.
(16) Balzani, V.; Campagna, S.; Denti, G.; Juris, A.; Serroni, S.; Venturi, M. *Acc. Chem. Res.* **1998**, *31*, 26−34.
(17) Bar-Haim, A.; Klafter, J.; Kopelman, R. *J. Am. Chem. Soc.* **1997**, *119*, 6197−6198.
(18) Kawa, M.; Fréchet, J. M. J. *Chem. Mater.* **1998**, *10*, 286−296.
(19) Kawa, M.; Fréchet, J. M. J. *Thin Solid Films* **1998**, *331*, 259−263.
(20) Jiang, D. J.; Aida, T. *J. Am. Chem. Soc.* **1998**, *120*, 10895−10901.
(21) Gilat, S. L.; Adronov, A.; Fréchet, J. M. M. *Angew. Chem., Int. Ed. Engl.* **1999**, *38*, 1422−1426.
(22) Adronov, A.; Gilat, S. L.; Fréchet, J. M. J.; Ohta, K.; Neuwahl, F. V. R.; Fleming, G. R. *J. Am. Chem. Soc.* **2000**, *122*, 1175−1185.
(23) Lor, M.; De, R.; Jordens, S.; Belder, G. D.; Schweitzer, G.; Cotlet, M.; Hofkens, J.; Weil, T.; Herrmann, A.; Müllen, K.; Auweraer, M. V. D.; Schryver, F. C. D. *J. Phys. Chem. A* **2002**, *106*, 2083−2090.
(24) Maus, M.; De, R.; Lor, M.; Weil, T.; Mitra, S.; Wiesler, U.-M.; Herrmann, A.; Hofkens, J.; Vosch, T.; Müllen, K.; Schryver, F. C. D. *J. Am. Chem. Soc.* **2001**, *123*, 7668−7676.
(25) Schenning, A. P. H. J.; Peeters, E.; Meijer, E. W. *J. Am. Chem. Soc.* **2000**, *122*, 4489−4495.
(26) Chrisstoffels, L. A. J.; Adronov, A.; Fréchet, J. M. J. *Angew. Chem., Int. Ed.* **2000**, *39*, 2163−2167.
(27) Xu, Z.; Moore, J. S. *Acta Polym.* **1994**, *45*, 83−87.
(28) Swallen, S. F.; Kopelman, R.; Moore, J. S.; Devadoss, C. J. *Mol. Struct.* **1999**, *485*, 585−597.
(29) Serin, J. M.; Brousmiche, D. W.; Frechet, J. M. J. *Chemm. Comm.* **2002**, *22*, 2605−2607.
(30) Weil, T.; Reuther, E.; Mullen, K. *Angew. Chem., Int. Ed.* **2002**, *41*, 1900−1904.
(31) Weil, T.; Reuther, E.; Beer, C.; Mullen, K. *Chem. Eur. J.* **2004**, *10*, 1398−1414.
(32) Devadoss, C.; Bharathi, P.; Moore, J. S. *J. Am. Chem. Soc.* **1996**, *118*, 9635−9644.
(33) Shortreed, M. R.; Swallen, S. F.; Shi, Z.-Y.; Tan, W.; Xu, Z.; Devadoss, C.; Moore, J. S.; Kopelman, R. *J. Phys. Chem. B* **1997**, *101*, 6318−6322.
(34) Minami, T.; Tretiak, S.; Chernyak, V.; Mukamel, S. *J. Lumin.* **2000**, *87*−*89*, 115−118.
(35) Kleiman, V. D.; Melinger, J. S.; McMorrow, D. *J. Phys. Chem. B* **2001**, *105*, 5595−5598.
(36) Palma, J.; Roitberg, A. E.; Krause, J. L. to be submitted.
(37) Tada, T.; Nozaki, D.; Kondo, M.; Yoshizawa, K. *J. Phys. Chem. B* **2003**, *107*, 14204−14210.
(38) Kirkwood, J. C.; Scheurer, C.; Chernyak, V.; Mukamel, S. *J. Chem. Phys.* **2001**, *114*, 2419−2429.
(39) Gaab, K. M.; Thompson, A. L.; Xu, J.; Martínez, T. J.; Bardeen, C. J. *J. Am. Chem. Soc.* **2003**, *125*, 9288−9289.
(40) Thompson, A. L.; Gaab, K. M.; Xu, J.; Bardeen, C. J.; Martínez, T. J. *J. Phys. Chem. A* **2004**, *108*, 671−682.
(41) Harcourt, R. D.; Scholes, G. D.; Ghiggino, K. P. *J. Chem. Phys.* **1994**, *101*, 10521−10525.
(42) Krueger, B. P.; Scholes, G. D.; Fleming, G. R. *J. Phys. Chem. B* **1998**, *102*, 5378−5386.
(43) Ortiz, W.; Roitberg, A. E.; Krause, J. L. *J. Phys. Chem. B* **2004**, *108*, 8218−8225.
(44) Ponder, J. W. *TINKER, Software Tools for Molecular Design*, version 3.6; Washington University: St. Louis, MO, 1998. The most updated version for the TINKER program can be obtained from J. W. Ponder's WWW site at http://dasher.wustl.edu/tinker.
(45) Allinger, N. L.; Yuh, Y. H.; Lii, J.-H. *J. Am. Chem. Soc.* **1989**, *111*, 8551−8566.
(46) Lii, J.-H.; Allinger, N. L. *J. Am. Chem. Soc.* **1989**, *111*, 8566−8575.
(47) Lii, J.-H.; Allinger, N. L. *J. Am. Chem. Soc.* **1989**, *111*, 8576−8582.
(48) Okuyama, K.; Hasegawa, T.; Ito, M.; Mikami, N. *J. Phys. Chem.* **1984**, *88*, 1711−1716.
(49) Okuyama, K.; Cockett, M. C. R.; Kimura, K. *J. Chem. Phys.* **1992**, *97*, 1649−1654.
(50) Borst, D. R.; Chou, S. G.; Pratt, D. W. *Chem. Phys. Lett.* **2001**, *343*, 289−295.
(51) Speiser, S. *Chem. Rev.* **1996**, *96*, 1953−1976.

(52) Turro, N. J. *Modern Molecular Photochemistry*; The Benjamin/Cummings Publishing Company, Inc.: Menlo Park, CA, 1978.
(53) Förster, T. *Ann. Physik.* **1948**, *2*, 55−75.
(54) Gronheid, R.; Hofkens, J.; Köhn, F.; Weil, T.; Reuther, E.; Müllen, K.; Schryver, F. C. D. *J. Am. Chem. Soc.* **2002**, *124*, 2418−2419.
(55) Köhn, F.; Hofkens, J.; Gronheid, R.; Kotlet, M.; Müllen, K.; Van der Auweraer, M.; Schryver, F. C. D. *ChemPhysChem* **2002**, *3*, 1005−1013.
(56) Cotlet, M.; Gronheid, R.; Habuchi, S.; Stefan, A.; Barbafina, A.; Müllen, K.; Hofkens, J.; Schryver, F. C. D. *J. Am. Chem. Soc.* **2003**, *125*, 13609−13617.
(57) Wong, K. F.; Bagchi, B.; Rossky, P. J. *J. Phys. Chem. A* **2004**, *108*, 5752−5763.
(58) Hirata, Y.; Okada, T.; Nomoto, T. *Chem. Phys. Lett.* **1998**, *293*, 371−377.
(59) Beeby, A.; Findlay, K.; Low, P. J.; Marder, T. B. *J. Am. Chem. Soc.* **2002**, *124*, 8280−8284.
(60) Sanrame, C., personal communication, 2004.
(61) Ferrante, C.; Kensy, U.; Dick, B. *J. Phys. Chem.* **1993**, *97*, 13457−13463.
(62) Jang, S.; Newton, M. D.; Silbey, R. *J. Phys. Rev. Lett.* **2004**, *92*, 218301.